Acousto-optical multiple interference switches

M. Beck
Paul-Drude-Institut für Festkörperelektronik, Hausvogteiplatz 5-7, D-10117 Berlin, Germany

M. M. de Lima, Jr.
Paul-Drude-Institut für Festkörperelektronik, Hausvogteiplatz 5-7, D-10117 Berlin, Germany and Materials Science Institute, University of Valencia, P.O. Box 22085, E-46071 Valencia, Spain

E. Wiebicke, W. Seidel, R. Hey, and P. V. Santos[a)]
Paul-Drude-Institut für Festkörperelektronik, Hausvogteiplatz 5-7, D-10117 Berlin, Germany

The authors introduce an alternative approach for acousto-optical light control based on the interference of light propagating through several waveguides, each subjected to a periodic refractive index modulation induced by a surface acoustic wave. The feasibility of the concept is demonstrated by the realization of an optical switch for arbitrary time intervals with an on/off contrast ratio of 20. © 2007 American Institute of Physics. [DOI: 10.1063/1.2768889]

The acousto-optical interaction provides a well-established process for controlling light beams in solids.[1] With the advent of integrated optics, approaches have been sought after to implement the required phase matching between the acoustic and optical waves propagating in waveguide (WG) structures. Examples are the acoustically induced coupling between neighboring WGs (Ref. 1) and the use of Umklapp scattering in photonic crystals.[2,3]

As an alternative approach, Gorecki *et al.* proposed the combination of surface acoustic waves (SAWs) with Mach-Zehnder interferometers (MZIs) for WG modulators.[4,5] Here, the strain field of a SAW impinging perpendicularly to one of the interferometer arms introduces a periodic modulation of the transmitted light. More recently, de Lima *et al.*[6] introduced an approach for acoustically driven MZI, where a single SAW simultaneously modulates the refractive index of both MZI arms with opposite phases, as illustrated in Fig. 1(a). The opposite phase modulation of amplitude ϕ_{max} per arm is achieved by simply spacing the WGs by an odd multiple of the half acoustic wavelength λ_{SAW}.

In this letter, we demonstrate an alternative concept for WG acousto-optical elements based on the modulation of several interferometer arms by a single SAW beam. These acousto-optic multiple interference devices (AOMIDs) provide integrated optics building blocks for functionalities such as switching, harmonic generation, and pulse shaping.[7] The feasibility of the AOMID concept is established by the realization of a WG on/off switch for arbitrary time periods.

The AOMID concept is an extension of the acoustically driven MZIs of Fig. 1(a) for a number $N_P \geqslant 2$ of WG arms connected in parallel.[8] The configurations for $N_P=2$ (corresponding to the simple MZI), $N_P=4$, and $N_P=8$ are illustrated in Figs. 1(a)–1(c). In each case, the single mode WGs (numbered by the index $p=1,\ldots,N_P$) are assumed to be identical and much narrower than λ_{SAW}. The WGs are aligned perpendicularly to the SAW propagation direction and displaced laterally so as to experience SAW phases differing by a multiple of $\varphi_{SAW}=2\pi/N_P$. The amplitude ϕ_{max} of the light phase shift upon propagation through the WGs is related to the WG length ℓ and to the refractive index modu-

lation δn induced by the SAW strain by $\phi_{max}=2\pi\delta n\ell/\lambda_L$, where λ_L is the light wavelength. The use of symmetric Y-splitters in Fig. 1 ensures unity transmission in the absence of a SAW. Under the previous assumptions, the transmission T_P of an AOMID with N_P arms becomes:

$$T_P^{(N_P)}[t] = \left| \frac{1}{N_P} \sum_{p=0}^{N_P-1} e^{i[\phi_{max}\,\sin(2\pi f_{SAW}t + p\varphi_{SAW})]} \right|^2, \quad (1)$$

where f_{SAW} is the SAW frequency. Figure 1(d) compares the time dependence of the transmission for AOMIDs with different number of arms. By an appropriate choice of ϕ_{max}, the transmission becomes strongly suppressed when the SAW is turned on, thus illustrating the operation as a switch for arbitrary on/off times.

The transmission suppression can be intuitively understood by taking into account that for symmetric devices (as the ones in Fig. 1) (i) any variation in the refractive index leads to a reduced transmission and that (ii) the transmission is invariant under shifts of the SAW phase by multiples of
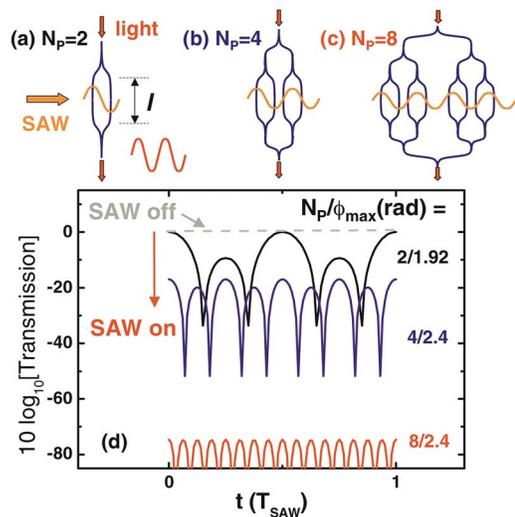

FIG. 1. (Color online) Acousto-optical multiple interference devices (AOMIDs) with (a) $N_P=2$, (b) $N_P=4$, and (c) $N_P=8$ arms. (d) Transmission for the given phase modulation ϕ_{max} for AOMID with $N_P=2$ ($\phi_{max}=1.92$ rad), $N_P=4$ ($\phi_{max}=2.4$ rad), and $N_P=8$ ($\phi_{max}=2.4$ rad).

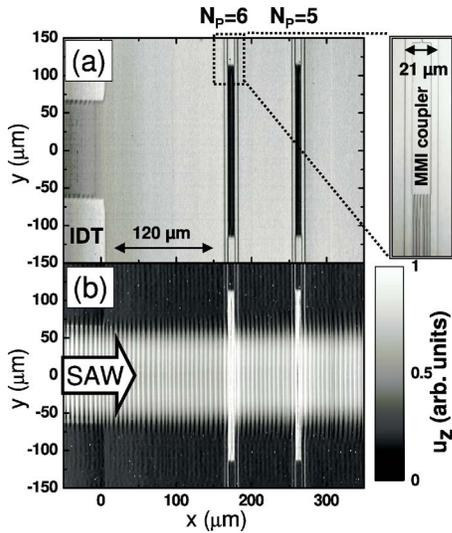a)Electronic mail: santos@pdi-berlin.de

FIG. 2. (Color online) (a) Optical and (b) interferometry micrographs of the vertical component u_z of the acoustic field of structures containing five- and sixfold AOMIDs. The inset shows the MMI coupler for the sixfold AOMID.

FIG. 3. (Color online) Symbols: Average (dc) transmission T_0 as a function of the rms voltage (V_{rf}) applied to the IDT for AOMIDs with $N_P=2$ (measured at $\lambda_L=910$ nm), $N_P=4$ ($\lambda_L=890$ nm), and $N_P=6$ ($\lambda_L=900$ nm). The dashed and solid lines display the calculated transmission for devices with symmetric and slightly asymmetric arms, respectively.

$2\pi/N_P$ [cf. Fig. 1(a)–1(c)]. As a result, when the refractive index of the arms is modulated by a SAW with frequency f_{SAW}, the transmission will reduce $2N_P$ times within a SAW cycle and only contains harmonics of the frequency $N_P f_{SAW}$. In fact, it can be shown that in the limit $N_P \rightarrow \infty$ the transmission becomes proportional to $J_0^2(\phi_{max})$,[7] where J_0 is the zero-order Bessel function, which vanishes for $\phi_{max}=2.405$ rad.

In order to demonstrate the previous concepts, we have fabricated AOMIDs with $N_P=2–6$ on an (Al, Ga)As WG sample grown on GaAs (100) by molecular beam epitaxy. The sample consists of a 300-nm-thick GaAs film forming the core of a surface WG deposited on a 1500-nm-thick $Al_{0.2}Ga_{0.8}As$ cladding layer. AOMIDs with $N_P=2$ and 4 were designed using symmetric Y-splitters to couple the input and output WGs to the 700-nm-wide WG arms. The devices with $N_P=3$, 5, and 6 employed multimode interference (MMI) couplers.[9] In this case, the width of the individual WGs was adjusted to ensure the same overall light phase shift through each WG arm. The AOMIDs were fabricated in two steps using contact optical lithography. First, the 150-nm-deep grooves delimiting the ridge WGs were produced by plasma etching. Subsequently, interdigital transducers (IDTs) for SAW generation were fabricated using a lift-off metalization process to structure a 60-nm-thick metal layer. The split-finger IDTs have an aperture of 120 μm and were designed for $\lambda_{SAW}=5.6$ μm (corresponding to $f_{SAW}\approx 520$ MHz). The radio-frequency (rf) power $P_{rf}=V_{rf}^2/R_{50}(R_{50}=50$ Ω) applied to the IDTs will be specified in terms of the nominal rms voltage V_{rf}. The fraction $r_p=0.14\pm0.03$ of P_{rf} converted to the acoustic mode was determined from rf-reflection measurements on the IDTs. Figure 2(a) shows a micrograph of the sample region with AOMIDs with $N_P=5$ and $N_P=6$, together with details of the MMI for the $N_P=6$ structure (inset). Note that both AOMIDs are driven by the same SAW beam.

An important consideration for AOMIDs regards the distribution of the acoustic fields across the WG structure, which was measured using a microscopic scanning Michelson interferometer. The two-dimensional plot of Fig. 2(b) displays the amplitude of the surface displacement u_z re-
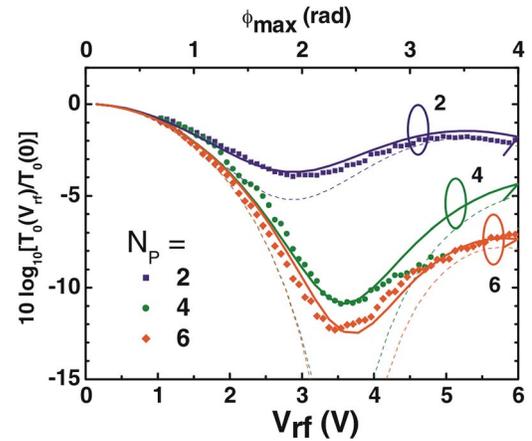
corded in the same area as in Fig. 2(a) for a particular SAW phase. The SAW wave fronts appear as finely spaced vertical lines separated by $\lambda_{SAW}=5.6$ μm. The SAW beam width corresponds closely to the aperture of the IDT of 120 μm and shows negligible attenuation (less than 5%) after traversing the five- and six-fold AOMIDs. The low attenuation is associated with the small ratio between the depth of the WG grooves and λ_{SAW} and clearly demonstrates that a single SAW beam can efficiently drive AOMIDs with a large number of arms.

The devices were optically characterized by coupling light into the input WG using a tapered fiber with a cylindrical lens on its tip. As light source, we used a superluminescent diode with a 50-nm-wide emission peak centered at the wavelength $\lambda=920$ nm. The fiber was mounted on a piezoelectrically controlled stage in order to allow for a fine positioning relative to the WG edge. The transmitted light was collected using a microscope objective (50$\times$) focused on the cleaved edge of the output WG and detected using an optical spectrometer.

The operation of AOMIDs as on/off switches is demonstrated in Fig. 3, which displays the time-averaged transmission $T_0(V_{rf})$ (normalized to the corresponding value in the absence of acoustic excitation) for devices with different numbers of arms. The light wavelength was slightly changed for the different devices in order to enhance the on/off contrast ratio by partially compensating for asymmetries in the WGs (see below). For $N_P=2$ (corresponding to a simple MZI), T_0 reaches a minimum of −6 dB for $V_{rf}=2.8$ V. The minimum transmission shifts to higher V_{rf} and reduces with N_P down to −12±1 dB for the sixfold device. The dashed lines show the dependence of T_0 on ϕ_{max} (upper scale) calculated for symmetric devices using a SAW-induced refractive index $\delta n(V_{rf})=r_n V_{rf}\sqrt{r_p/2R_{50}\ell}$. Here, the factor 2 in the denominator accounts for the bidirectionality of the IDT, i.e., the fact that the IDT emits both along the positive and negative x directions. The acousto-optical coupling factor r_n was obtained from the photoelastic coefficients of GaAs (Ref. 10) and from the the depth dependence of the SAW strain fields.[11] Further details about the calculations will be given in Ref. 7. In order to fit the position of the minima, we use photoelastic coefficients 15% higher than those reported for
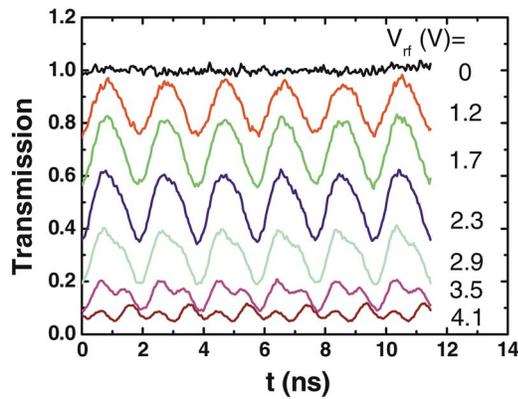
FIG. 4. (Color online) Time-resolved traces of the periodic transmission of a sixfold AOMID measured at $\lambda_L = 910$ nm for different rf-voltages (V_{rf}) applied to the IDT.

$\lambda = 1$ μm.[10] The latter is attributed to the enhanced acousto-optical coupling close to the GaAs gap.

The calculations reproduce well the voltage dependence of the transmission for small phase amplitudes ϕ_{max}. For phases near 2.4 rad, however, they predict a much stronger suppression of the transmission than the ones measured for devices with $N_P \geq 4$. In order to address this discrepancy, we have carried out time-resolved (time resolution of 600 ps) transmission measurements by selecting a narrow (10 nm) spectral band and detecting the light using an avalanche photodiode. Figure 4 shows time-resolved transmission traces recorded on an AOMID with six arms for different V_{rf}. In agreement with Fig. 3, the average transmission reduces with V_{rf} and reaches a minimum of approximately 5% (=13 dB) for $V_{rf} = 4$ V.[12] The transmission reduction is accompanied by pronounced oscillations at the first (for $1.2 < V_{rf} < 2.9$ V) and second harmonics (for 2.9 V $< V_{rf}$) of the SAW frequency. These harmonics, which are not expected for symmetric AOMIDs, are attributed to asymmetries of the WG arms arising from differences in the optical length ($\delta\ell$) or transmission of the individual WGs. In order to illustrate this behavior, the solid lines in Fig. 3 were calculated assuming a

maximum path difference $\delta\ell_{max}^{(opt)} = 140$ nm between any of the arms. For devices with $N_P > 2$, there are different ways of distributing the path differences between the arms. In the calculations, we simply assumed that it increases linearly from 0 to $\delta\ell_{max}^{(opt)}$ with the distance from the transducer. This simple model reproduces reasonably well the transmission over a wide range of phases. Since $\delta\ell_{max}^{(opt)}/n \sim 40$ nm is comparable to the tolerances of the employed optical lithography, much higher on/off contrast ratios are expected for an improved fabrication process.

In conclusion, we have demonstrated the feasibility of the AOMID concept in realizing an on/off switch with a high contrast ratio.

[1]A. Korpel, *Acousto-Optics* (Dekker, New York, 1997).

[2]W. L. Liu, P. S. J. Russell, and L. Dong, Opt. Lett. **22**, 1515 (1997).

[3]P. V. Santos, J. Appl. Phys. **89**, 5060 (2001).

[4]C. Gorecki, E. Bonnotte, H. Toshioshi, F. Benoit, H. Kawakatsu, and H. Fujita, Proc. SPIE **3098**, 392 (1997).

[5]C. Gorecki, F. Chollet, E. Bonnotte, and H. Kawakatsu, Opt. Lett. **22**, 1784 (1997).

[6]M. M. de Lima, Jr., M. Beck, R. Hey, and P. V. Santos, Appl. Phys. Lett. **89**, 121104 (2006).

[7]M. Beck, M. M. de Lima, Jr., and P. V. Santos, J. Appl. Phys. (to be published).

[8]Similar functionalities can be achieved by connecting several interferometer arms in series, see Ref. 7.

[9]L. B. Soldano, F. B. Veerman, M. K. Smit, B. H. Verbeek, A. H. Dubost, and E. C. M. Pennings, J. Lightwave Technol. **10**, 1843 (1992).

[10]*Elastic, Piezoelectric, Pyroelectric, Piezooptic, Electrooptic Constants and Nonlinear Dielectric Susceptibilities of Crystals*, Landolt-Börnstein Vol. 11, edited by K. H. Hellwege and A. M. Hellwege (Springer, Heidelberg, 1979).

[11]M. M. de Lima, Jr. and P. V. Santos, Rep. Prog. Phys. **68**, 1639 (2005).

[12]V_{rf} for minimum transmission is higher than in Fig. 3 due to the lower efficiency of the IDT.